




# Ballistic power: GPS-derived measurements suitable for the real-time monitoring of neuromuscular fatigue during repeated sprints

Eamon McGleenan<sup>1</sup> , Samuel D. T. Grant<sup>1</sup>, Lisa M. McFetridge<sup>1</sup>, Jack C. J. Brown<sup>1</sup>, Joseph W. Shaw<sup>2,3</sup>, Tiago de Melo Malaquias<sup>4,5</sup>, Ruth Montgomery<sup>4</sup>, and David B. Jess<sup>1</sup>

## Abstract

Power-force-velocity (*PFv*) measurements have traditionally been employed to characterize the limits of an athlete's neuromuscular system. However, in more recent years, there has been growing interest in whether *PFv* metrics can also be used to define and assess training outcomes, e.g., as an indicator of performance and/or neuromuscular fatigue. Here we assess performance in a repeated sprint ability (*RSA*) test using traditional *PFv* measurements, alongside two novel metrics: ballistic power ( $P_B$ ) and the *Fv*-offset, with the changes observed attributed to neuromuscular fatigue. Twenty-four physically active males (age =  $26.08 \pm 6.84$  years) undertook the *RSA* test, consisting of 3 sets of  $5 \times 50$  m maximal sprints, with each participant wearing a STATSports Apex Pro series unit to track their motion. Mixed-effect models show how power-related metrics have the largest reduction due to fatigue compared to their force and velocity counterparts, with  $P_B$  showing the largest decrease of  $\sim 31.8\%$  ( $-40.2 \leq P_B(\% \text{ change}) \leq -23.4$ , 95% CI, Cohen's  $d = 1.60$ ) across the *RSA* test performed. We demonstrate that ballistic power,  $P_B$ , is the most reactive metric to athlete fatigue amongst the considered values. The described methods provide a promising, feasible tool for field-based monitoring of fatigue using routine GPS data.

## Keywords

Global positioning system, power-force-velocity relationships

## Introduction

Monitoring acute neuromuscular fatigue – here defined as “an exercise-induced reduction in the force/power-generating capacity of a muscle or muscle group”<sup>1</sup> – is important for sports science and medicine practitioners to inform decisions around training load and match selection. Over days and weeks, this is often achieved through routine subjective (e.g., wellness questionnaires) and objective (e.g., counter movement jump, heart rate variability) measures. The value and validity of such measures, however, has been questioned in review articles that instead call for more practical field-measures derived from training and match data.<sup>2,3</sup> Furthermore, such approaches are not practical in real-time (i.e., during training or match-play), where the insights are of the greatest value.

The widescale uptake of global positioning systems (GPS) has provided professional sports teams with a wealth of spatiotemporal data relating to player-movement. To date, the majority of methods to estimate neuromuscular

status using spatiotemporal data have taken an indirect approach, whereby an athlete's change in status is modelled as a linear function of the cumulative volume of a given

Reviewers: Adam Lipcak (Masayk University, Czech Republic)  
Carlos Serrano (European University, Spain)

<sup>1</sup>Predictive Sports Analytics, School of Mathematics and Physics, Queen's University Belfast, Belfast, Northern Ireland, BT7 1NN, UK

<sup>2</sup>Irish Rugby Football Union, Dublin, Ireland

<sup>3</sup>Faculty of Sport, Technology and Health Sciences, St Mary's University, London, UK

<sup>4</sup>STATSports Group Limited, Drumalane Mill The Quays, Newry, Northern Ireland, BT35 8QS, UK

<sup>5</sup>Al Qadsiah Football Club, Al Khobar, Saudi Arabia

## Corresponding author:

Eamon McGleenan, Predictive Sports Analytics, School of Mathematics and Physics, Queen's University Belfast, Belfast, Northern Ireland, BT7 1NN, UK.

Email: emcgleenan04@qub.ac.uk

external load metric (e.g., total distance, high-speed running distance, sprint count, etc.) between periods of play in competitive events.<sup>4-7</sup> This approach, however, fails to account for (i) intra- and inter-athlete variation in the response to a given external load, and (ii) the effect of fatiguing actions that are not quantified in external load metrics (e.g., scrummaging in rugby). Subsequently, it is unsurprising that such relationships are limited in their predictive ability ( $R^2 < 0.45$ <sup>8</sup>), with recent literature suggesting there are advantages in adopting approaches that reflect the physiological, mechanical, and neuromuscular aspects more clearly.<sup>9</sup>

Recently, several studies have investigated the viability of using training or match-derived GPS data to directly measure qualities relating to physical performance. Morin et al.,<sup>10</sup> for example, demonstrated that force-velocity profiles could be reliably estimated using GPS data from multiple training sessions. Additionally, across a simulated soccer match, Snyder et al.<sup>11</sup> observed a decline in traditional GPS metrics over time, such as those associated with high-speed running, accelerations per minute, and decelerations per minute.

Furthermore, GPS metrics can also be utilized to generate power-velocity ( $Pv$ ) and force-velocity ( $Fv$ ) relationships (collectively defined as ' $PFv$ '), which are useful in the benchmarking of ballistic movements.<sup>12-14</sup> Here, ballistic movements are defined as any movement that exhibits high and near-maximal velocities and accelerations over a short period of time (see, e.g., Morin & Samozino<sup>15</sup> for more information), hence may be significantly affected by acute neuromuscular fatigue, here defined as "a reduction (induced by exercise) in the maximal voluntary force that a muscle or group of muscles can generate".<sup>16</sup> As such, repeated sprint ability ( $RSA$ ) has been a focus of recent investigations.<sup>17-20</sup>  $RSA$  has also been explored in the context of endurance athletes, where in some cases, intense bursts of concentrated effort are separated by short recovery periods,<sup>21</sup> meaning  $RSA$  is a physiological requirement across a wide range of sports.

In laboratory or field-based  $RSA$  testing protocols, fatigue is typically identified through a reduction in an athlete's maximal or mean speed, or a decrease in their peak power or total work done during repeated sprints.<sup>22</sup> The total force production capability of an athlete, and their technical ability to effectively apply the necessary force, are altered during multiple sets of repeated sprints, with the latter often believed to be the dominant effect.<sup>23</sup> As a result,  $PFv$  profiling is commonly presented as a tool to assess the ability of an athlete's neuromuscular system to produce power; indeed maximal muscular power is defined and limited by the underlying force-velocity relationship.<sup>24</sup> However, previous studies have cited the necessity to examine the usefulness of these metrics in orienting and assessing training outcomes<sup>25</sup> and highlighted the necessity for further investigation into how these approaches can be used to improve sprint performance.<sup>26</sup>

Hence, the creation of reliable and robust methodologies to apply  $PFv$  analysis to widespread GPS data collection would provide significant insight into the  $RSA$  of an athlete and may better inform training prescriptions and practices. The aim of the present study is to put forward a proof-of-concept methodology to quantitatively assess an athlete's capacity for repeatedly performing explosive movements, using changes in  $PFv$  outputs. In a multi-set repeated sprint ability ( $RSA$ ) test, it was hypothesized that multiple indicators of neuromuscular fatigue would be observed in both intra- and inter-set analyses. The extent and comparison of these neuromuscular fatigue indicators are the main focus of this study, as well as identifying which of these metrics are most sensitive to neuromuscular fatigue and how readily they may be applied by sports scientists and strength and conditioning practitioners to real-time sporting environments.

## Materials and methods

### Research design

The procedure of the  $RSA$  test required each participant to complete 3 sets of sprints, with each set consisting of 5 × 50 m sprint intervals. During each set, individual sprint repetitions commenced every 30 seconds with passive recovery between efforts and sets, as this recovery modality has not been shown to influence repeated-sprint performance (as indicated by sprint time and blood acid-base responses<sup>27</sup>), thereby ensuring that the running load itself was the principal driver of neuromuscular fatigue and subsequent intraset performance degradation. Following the completion of a sprint set, a 2 minutes and thirty seconds (2:30) recovery period was provided to each athlete. All subjects completed the  $RSA$  test collectively. The subjects received a familiarization document containing the procedure of the  $RSA$  test on the morning of the day it was carried out. The  $RSA$  test was performed following a routine warm up, 4 days following the team's most recent game, and 4 days before the team's next game. The test takes approximately 15 minutes and covers a distance of 750 m. Players are instructed to complete every repetition at maximum effort. The test was performed after a standard team warm up activity that involves low intensity running, sport specific drills, followed by dynamic and static stretching to benefit muscle flexibility following the commonly applied Raise, Activate, Mobilize, and Potentiate (RAMP) warm-up protocols.<sup>28</sup>

This protocol was designed to induce measurable neuromuscular fatigue within a standard set and repetition structure that is consistent with mainstream literature,<sup>29</sup> although longer (50 m) sprint distances were selected to ensure there is a meaningful fatigue response from each athlete. The  $RSA$  structure chosen also reflects the high-speed and sprint running demands of field sports, such as Gaelic football,<sup>30</sup>

soccer,<sup>31</sup> and rugby union.<sup>32</sup> The *RSA* test protocol was designed to ensure sufficient fatigue develops within a controlled, sport-specific format.

### Subjects

Twenty-four male subjects aged between 19 and 43 ( $26.08 \pm 6.84$  years) voluntarily took part in this study. All participants are physically active, typically training between 2 – 3 times per week, and compete at the sub-elite level of an invasive team sport. Written, informed consent was obtained from the participants and the study was approved by the Engineering and Physical Sciences Faculty Research Ethics Committee of Queen's University Belfast (reference number: EPS 24\_48).

### Procedures

The hardware and software used to gather data were both developed by the Northern Ireland company STATSports Group Limited. STATSports Apex Pro series units were utilized<sup>1</sup>, while initial data import and validation was performed using the STATSports Sonra software<sup>2</sup>. The data gathered was exported in its raw format into a series of comma-separated values (CSV) files, which allowed further analysis through various customized computational methods. Specifically, Python 3<sup>33</sup> was used as the primary programming language for the data analyses undertaken in the present study.

STATSports Apex Pro series units have been validated for data reliability and accuracy independently through the FIFA Quality Programme, against the industry gold standard Vicon motion capture system.<sup>34</sup> In measuring linear and simulated team sport running, GPS-based devices (such as the STATSports Apex Pro series units) with a sampling frequency of 10 Hz are the most accurate and reliable to date.<sup>35</sup> As a result, the technology embedded within the STATSports Apex Pro series units is sufficient to provide reliable measurements of horizontal (i.e., within the plane of the training surface) *PFV* values across individual samples of maximal effort sprints.<sup>36</sup> The number of satellites connected ranged from 14 – 20 (mean = 17) throughout the *RSA* test, with the Horizontal Dilution of Precision (HDOP) value measured to be  $0.41 \pm 0.07$ , allowing for accurate horizontal position calculations from the GPS devices.<sup>37</sup>

### Statistical analysis

The analysis carried out for this study used the raw (i.e., unprocessed and unfiltered) CSV file exports provided by the Sonra software, with the data imported into Python 3<sup>33</sup> using the Pandas library.<sup>38</sup> Note that for the purposes of our analysis, the use of the terms 'speed' and 'velocity' are interchangeable due to the fact that the sprints

performed were uni-directional. Of course, future studies that may incorporate curvi-linear running patterns may need to segregate individual velocity vector components or utilize true speed values through the extraction of velocity magnitudes.

The starting point of each athlete's sprint was identified by the timestamp when their velocity first increased above a nominal low-speed (i.e.,  $v > 0.25 \text{ m s}^{-1}$ ) threshold. A low-speed threshold was chosen over a completely stationary value (i.e.,  $v = 0 \text{ m s}^{-1}$ ) to avoid incorrect sprint labeling when an athlete shuffles their body position in preparation for the sprint. As such, the first timestamp corresponds to the minimum velocity value,  $v_{\min}$ , associated with the sprint event. The end of the running repetition was pinpointed by the timestamp when the athlete's velocity decreased below  $1 \text{ m s}^{-1}$ . The running repetition motion was subsequently isolated and extracted for further study, with an example time series documenting an athlete's velocity over the duration of a single repetition displayed using blue datapoints in Figure 1. The specific start/end thresholds were maintained throughout the entirety of the data processing, which is a necessity to ensure consistency and repeatability of any time series analyses.<sup>39</sup>

Speed values were sampled at a rate of 10 Hz. To suppress high-frequency fluctuations (i.e., those that are much more rapid than the sprint evolutionary timescales; see Figure 1), a Butterworth filter (2 Hz, low-pass<sup>40</sup>) was employed to smooth the GPS-derived velocity values by suppressing measurement fluctuations with timescales less than 0.5 s. Butterworth filters are commonly applied to improve the estimation of measures affected by high-frequency GPS inaccuracies.<sup>41–43</sup> Previously, a 2 Hz low-pass Butterworth filter was shown to correlate strongly with Vicon data, which is considered to be the 'gold-standard' in motion analysis systems.<sup>44</sup>

From the Butterworth-smoothed velocity values, the maximum sprint speed was extracted. From this, the end of the sprint was identified by the timestamp when the athlete's velocity first dropped below 70% of their maximum speed achieved during the repetition. Note that 70% is an arbitrary value, but it is chosen (and remains fixed throughout the analyses) to ensure subsequent polynomial fitting is not negatively affected when the athlete's speed reduces, which is a period not based on maximal sprint technique and is often represented by unpredictable deceleration rates and occasional anomalous accelerations as the subjects prepare for the next repetition. Hence, the sprint interval is defined as the datapoints contained between the first timestamp when the athlete's velocity rises above  $0.25 \text{ m s}^{-1}$ , through to the point when the athlete's velocity drops below 70% of their maximum sprint speed. A fourth order polynomial is applied to the smoothed velocity data defined by the sprint interval. From this, the acceleration is subsequently computed (green line in Figure 1<sup>45</sup>). Finally, only datapoints with positive acceleration values are selected for

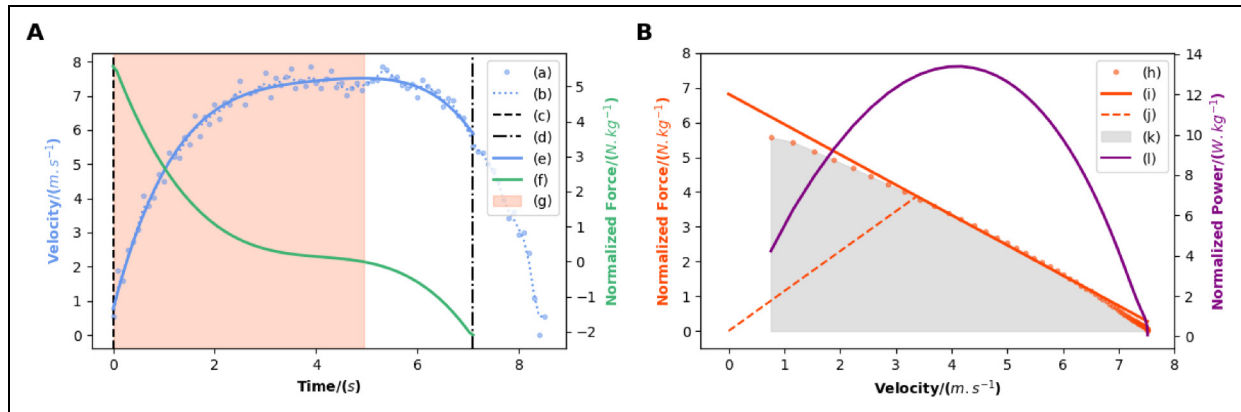


**Figure 1.** Panel A shows velocity ( $\text{m s}^{-1}$ ) and normalized force ( $\text{N kg}^{-1}$ ) as a function of time (seconds) for 1 repetition from a single athlete during the RSA test. As indicated in the legend, (a) is the raw velocity time series, (b) is the Butterworth filtered values of (a), (c) and (d) are vertical lines that represent the times at which the minimum speed threshold ( $0.25 \text{ m s}^{-1}$ ) and where the speed drops to below 70% of the maximum speed reached within the sprint repetition, respectively, are reached. (e) is a fourth order polynomial fit of the Butterworth-filtered velocity data between the timestamps represented by (c) and (d), and (f) is the corresponding normalized force ( $\text{N kg}^{-1}$  or  $\text{m s}^{-2}$ ) estimated from the polynomial fit. Finally, (g) highlights the data where the acceleration value is  $>0 \text{ m s}^{-2}$ , which is subsequently used in the *PV* analysis. Panel B displays the normalized force (h;  $\text{N kg}^{-1}$ ) and the normalized power (i;  $\text{W kg}^{-1}$ ) as a function of velocity for the data contained within the shaded region (g) in A. (i) is the linear fit of (h) excluding data within the first 30% and last 10% of the range of velocity values (outside of this exclusion area curved sections are visible, so these thresholds consistently ensure only straight sections are modeled using linear lines of best fit), while (j) is the shortest perpendicular distance from (i) to the origin. (k) is the area underneath (h) and represents the ballistic power (see Equation 1).

further study since this data is representative of the ballistic (i.e., positively accelerating) phase of the sprint. The shaded orange region within panel A of Figure 1 highlights the datapoints showcasing positive acceleration values, which define instances when positive work is being performed by the athlete (i.e., negating intervals of negative work, which would be considered non-physical).

We note that recent work has shown how the acceleration phase of a sprint event can be divided up into 3 distinct phases,<sup>46</sup> which has since driven forward a number of further sprint-related studies.<sup>47</sup> Hence, the fitting of our velocity time series with a low-order polynomial is consistent with the biomechanical theory put forward by Nagahara et al.,<sup>46</sup> hence enabling the accurate mapping of the macroscopic velocity/acceleration profiles of athletes' sprints, which is visible through examination of the solid blue and green lines (labeled 'e' and 'f', respectively) in Figure 1, panel A. We must note that our analysis does not rely on the accurate definition of a sprint entry/exit speed, since in our controlled *RSA* test the participants commenced each sprint from an approximate standing start. Furthermore, our selected sprint exit speed of 70% of each athlete's maximum sprint speed is arbitrary and only used to extract the main sprint effort from the bulk of the deceleration phase, which may (as noted above) contain unpredictable deceleration rates and occasional anomalous accelerations as the subjects prepare for the next repetition. However, future applications of this approach (e.g., where the subjects are not commencing their sprints from rest) may need to incorporate more stringent sprint entry

identifications, such as using a threshold of 75% of the maximal velocity, which is in-line with current literature that considers sprint events from a kinematic viewpoint.<sup>48</sup>

Next, it is possible to display how both the athlete's force,  $F$ , and power,  $P$ , vary as a function of sprint speed. Here, the athlete power is defined using standard convention<sup>49</sup> as  $P = Fv = mav$ , where  $m$  is the mass of the athlete. For the purposes of ensuring future cross-referencing compatibility with data obtained from different athletes, the force and power values for each athlete are normalized by their respective masses. In practice, mass-normalized forces are analogous to raw acceleration values, since through Newton's second law of motion ( $F = ma$ ), acceleration can be made the subject to provide  $a = F/m$ . This means that subsequent calculations employing the mass-normalized force values are also, by definition, mass-normalized (e.g., power). This provides a (mass-)normalized force in units of  $\text{N kg}^{-1}$ , which is identical to acceleration (i.e.,  $\text{m s}^{-2}$ ), and a (mass-)normalized power in units of  $\text{W kg}^{-1}$ .

The resulting normalized force-velocity ( $Fv$ ) and power-velocity ( $Pv$ ) curves are shown in panel B of Figure 1 using orange datapoints and purple lines, respectively. The extreme values of speed ( $v_{\text{min}}$  and  $v_{\text{max}}$ ) and maximum acceleration ( $a_{\text{max}}$ ) can easily be recovered from panel B of Figure 1 through examination of the extrema of the plotted orange ( $Fv$ ) datapoints. Similarly, the maximum value of power ( $P_{\text{max}}$ ) can also be uncovered from panel B of Figure 1, which can be visualized as the turning point (i.e., peak) of the  $Pv$  curve (purple line in Figure 1).

**Ballistic Power and the  $Fv$ -offset.** In addition, we define a new metric, ballistic power ( $P_B$ ), through the mathematical relationship,

$$P_B = \int_{v_{\min}}^{v_{\max}} F \, dv \text{mm} (\forall F > 0), \quad (1)$$

which can be visualized as the area under the  $Fv$  curve (shaded grey in panel B of Figure 1). Here, the ballistic power is the integration of normalized force ( $\text{N kg}^{-1}$ , or equivalently acceleration in  $\text{m s}^{-2}$ ) with respect to velocity over the initial period of positive acceleration during a sprint event and was calculated using the *np.trapz* function, which integrates along the given domain using the composite trapezoidal rule.<sup>45</sup> Thus, the ballistic power incorporates significantly more data within an isolated sprint when compared to, e.g., maximal values of power that only use isolated (or singular) points of reference. As such, the ballistic power of an athlete represents dynamic movement that generates positive acceleration (i.e., for all athlete forces greater than zero;  $\forall F > 0$  in Equation 1), hence increasing the velocity of associated movements.

Another complementary metric can also be derived from the  $Fv$  curve shown in panel B of Figure 1. Here,  $d_{Fv}$  (or the  $Fv$ -offset), is defined as the shortest perpendicular distance from the origin of the plot (i.e.,  $[0 \text{ m s}^{-1}, 0 \text{ N kg}^{-1}]$ ) to a linear fit through the corresponding  $Fv$  data points. However, to ensure power values at the extrema of the velocity range (i.e., close to either  $0 \text{ m s}^{-1}$  or the maximum sprint speed,  $v_{\max}$ ), where athlete performance is at its physiological limits, do not detrimentally impact the quality of the linear fit, we only fit velocities in the interval spanning 30% – 90% of  $v_{\max}$ . This range was chosen to ensure that the linear fit excludes both the initial and final phases of the  $Fv$  profile where non-linearities are observed. By using 30 – 90% of the  $v_{\max}$  range, the influence of profile curvature is reduced, allowing a linear fit to be applied that better reflects previously studied  $Fv$  relationships.<sup>10,23,25</sup> The resulting linear line of best fit is shown in panel B of Figure 1 using a solid orange line, where the associated gradient is denoted by  $S_{Fv}$ . To calculate the  $S_{Fv}$  value, we applied linear regression to the mass-normalized forces, as a function of velocity, across the range of speed values (30 – 90% of  $v_{\max}$ ) using the *numpy.polyfit* package within the Python 3 programming environment. The gradient returned represents the  $S_{Fv}$  metric, with the regression line subsequently evaluated across the full range of velocities using the *numpy.polyval* package, as shown by the solid orange line (labeled ‘i’) in Figure 1, panel B.

Importantly, the length of the orange dashed line in panel B of Figure 1 represents the  $d_{Fv}$  metric, which is the shortest (i.e., perpendicular) distance from the origin to the line of best fit through the  $Fv$  data. Note, the orange dashed line in panel B of Figure 1 does not visually appear to intersect perpendicularly with the solid orange line, which is simply

a consequence of the rectangular aspect ratio used for displaying the plotted information.

Interestingly, we propose that the maximum theoretical values of speed and acceleration (or mass-normalized force) can be recovered from panel B of Figure 1 as the  $x$ - and  $y$ -axis intercept points, respectively, of the solid orange line of best fit through the  $Fv$  datapoints. It is clear from panel B of Figure 1 that the theoretical maximum sprint speed and acceleration are larger than what the athlete achieved during the sprint itself. However, this is to be expected as the maximum theoretical values will neglect physiological and biomechanical challenges associated with initial traction, air resistance, surface friction, running technique, etc.<sup>12,46,50–52</sup>

The importance of the  $Fv$ -offset ( $d_{Fv}$ ) metric cannot be overstated, since different athletes may produce the same overall slope,  $S_{Fv}$ , of their  $Fv$  data, yet may have vastly different  $F_{\max}$  and  $v_{\max}$  values. Hence, the  $d_{Fv}$  metric is a useful way of differentiating the maximal force/velocity values of athletes who may have the same  $Fv$  slope. For example, if two athletes have the same  $S_{Fv}$  value, then the athlete with the larger  $d_{Fv}$  metric will be the one with greater  $F_{\max}$  and  $v_{\max}$  ratings. As such, the  $d_{Fv}$  metric provides an indication of variance in performance amongst those with the same  $Fv$  slope ( $S_{Fv}$ ).

## Results

Table 1 provides definitions for a number of parameters that can be readily extracted from the data products showcased in Figure 1. In addition to the metric definitions, in Table 1 we also provide the corresponding mean value (complete with its associated standard deviation), alongside the observed maximum and minimum values for each metric obtained from the participating athletes.

### Changes in power, force, and velocity outputs during the RSA test

Panel B of Figure 1 shows normalized force and power as a function of velocity. The turning point (or peak) of the normalized power curve provides the value for the maximum sprint power,  $P_{\max}$ . We found that the value of  $P_{\max}$  occurs at progressively lower speeds throughout the *RSA* test. For example, in Repetition 1, the peak power across all athletes occurred at  $4.46 \pm 0.17 \text{ m s}^{-1}$ , whereas in Repetition 15 the peak power occurred at  $3.99 \pm 0.22 \text{ m s}^{-1}$ . The kurtosis of the power-velocity curves throughout the *RSA* test was negative, with values in the range of  $-1.0$  to  $-1.5$ . Across the evolution of the *RSA* test, the skewness of the power-velocity curves followed a slight downward trend, with a range of values spanning  $-0.6$  to  $1.0$ , with the majority of values falling between  $0.0$  –  $0.2$ .

Figure 2 displays the relative percentages for all 6 metrics defined in Table 1 across the full 15 repetitions of

**Table 1.** Metrics investigated in this study, including their denotation, unit, definition, mean value presented with standard deviation as well as maximum and minimum values.

Metric	Unit	Definition	Mean Value	Max Value	Min Value
$v_{\max}$	$\text{m s}^{-1}$	Maximum velocity achieved within a repetition of the RSA test	$7.24 \pm 0.58$	8.95	5.59
$F_{\max}$	N	Maximum mass-normalized force (i.e., $\text{N kg}^{-1}$ or $\text{m s}^{-2}$ ) achieved within a	$4.83 \pm 0.62$	6.87	2.05
	$\text{kg}^{-1}$	repetition of the RSA test			
$P_{\max}$	W	Maximum power achieved within a repetition of the RSA test	$11.80 \pm 1.88$	18.17	5.03
	$\text{kg}^{-1}$				
$P_B$	W	Ballistic power provided by the area underneath the $F_v$ curve for each	$18.10 \pm 3.55$	30.33	7.28
	$\text{kg}^{-1}$	repetition of the RSA test			
$S_{Fv}$	$\text{s}^{-1}$	Slope of the linear line of best fit applied to the $F_v$ datapoints for each	$-0.76 \mp 0.10$	-0.27	-1.04
		repetition of the RSA test			
$d_{Fv}$	N/A	Shortest perpendicular distance from the origin to the linear line fitted to the	$4.72 \pm 0.49$	6.02	2.43
		$F_v$ datapoints ( $F_v$ -offset)			

Notes: RSA = Repeated Sprint Ability;  $F_v$  = Force Velocity.

the RSA test. Here, the  $v_{\max}$ ,  $F_{\max}$ ,  $P_{\max}$ ,  $P_B$ ,  $S_{Fv}$ , and  $d_{Fv}$  metrics for each repetition were normalized by their own respective mean value obtained in the very first repetition to provide an easier way to visualize the percentage changes for each metric as a function of repetition number.

All metrics (except for  $S_{Fv}$ ) have the largest mean value occurring in the first repetition, with a general percentage decline found across the entire RSA test. There were noticeable recoveries between sets (i.e., between repetitions 5 – 6 and 10 – 11) when the athletes have an extra 02:30 recovery time available to them. The ballistic power,  $P_B$ , responded more to sprint-induced fatigue than the peak power ( $P_{\max}$ ) value, with a decrease of 31.8% ( $-40.2 \leq P_B(\% \text{ change}) \leq -23.4$ , 95% CI, Cohen's  $d = 1.60$ ) found in  $P_B$  across the RSA programme, compared with just a 29.3% ( $-35.9 \leq P_{\max}(\% \text{ change}) \leq -22.7$ ), 95% CI, Cohen's  $d = 1.87$ ) decrease in  $P_{\max}$ . The Cohen's  $d$  values of 1.60 and 1.87 for  $P_B$  and  $P_{\max}$  distributions, respectively, highlight a strong statistical effect between the first and last repetitions of the RSA test, with the  $P_B$  metric showing the largest overall percentage change.

The maximum repetition sprint speed ( $v_{\max}$ ; blue line in Figure 2) displayed the largest recovery between sets, with the start of sets 2 (repetition 6) and 3 (repetition 11) recovering to values of 97.3% and 94.2%, respectively, of the initial maximum. The two power measurements in Figure 2,  $P_{\max}$  (green line) and  $P_B$  (red line), showed greater relative decline during the entire RSA test, with  $P_B$  dropping to 68.2% of its opening maximum in repetition 14.

### Comparison of traditional and novel PFv metrics

Figure 3 displays the maximum force ( $F_{\max}$ ; panel A), maximum power ( $P_{\max}$ ; panel B), and ballistic power ( $P_B$ ; panel C) as a function of maximum sprint speed ( $v_{\max}$ ) for each athlete across all repetitions of the RSA test. We found that the  $F_{\max}$ ,  $P_{\max}$ , and  $P_B$  metrics all increased in an

approximately linear manner as a function of maximum athlete speed, independent of the individual athlete or repetition number of the RSA test. The linear relationship between  $P_{\max}$  and  $v_{\max}$  was found to have the strongest correlation of the 3 plots shown in Figure 3 (panel B), achieving a coefficient of determination of  $R^2 = 0.73$ , while the  $F_{\max}$  and  $P_B$  panels have coefficients of determination equal to  $R^2 = 0.42$  and  $R^2 = 0.54$ , respectively.

To more thoroughly investigate the relationships between  $F_{\max}$ ,  $P_{\max}$ , and  $P_B$  as a function of  $v_{\max}$ , linear mixed effects models were fitted using the *nlme* package in the R statistical software package (version 4.5.1<sup>53,54</sup>), specifying  $F_{\max}$ ,  $P_{\max}$ , and  $P_B$  as the corresponding response variables and  $v_{\max}$  as a fixed covariate in each model. Through the incorporation of random intercept terms, these sophisticated models accounted for the natural correlation within the repeated measurements of athletes to uncover the true underlying relationships within RSA test data.

The degree of correlation accounted for through the inclusion of random effects terms was calculated using the Intraclass Correlation Coefficient (ICC<sup>55</sup>), with values greater than 10% generally indicating the requirement of mixed effects models for improved performance compared to standard linear regression.<sup>56</sup> Akaike Information Criterion (AIC) and Bayesian Information Criterion (BIC) were additionally utilized to assess the fit of the model and showed agreement with the ICC, indicating the mixed effects model provided a better fit to the data compared to a standard linear model. Standardized residuals for each model also showed a random scattering when plotted, indicating the models' assumptions about the variance and linearity of the data were upheld. QQ plots and histograms were utilized to assess the normality assumptions of the residuals and random intercepts, each showing no large departures from normality.

As displayed in Figure 3, both  $F_{\max}$  and  $P_{\max}$  demonstrated strong individual correlations, with ICC values of

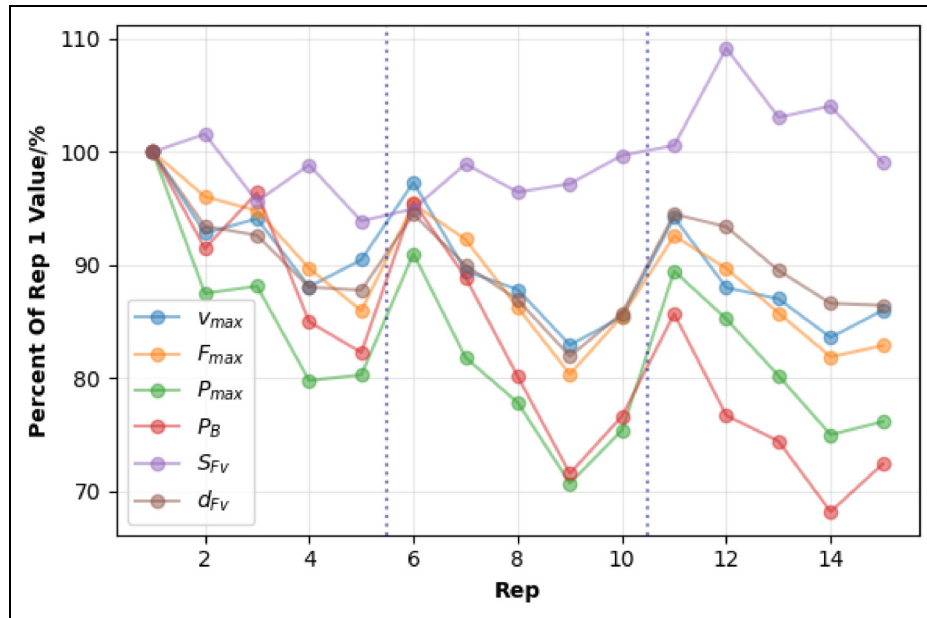


**Figure 2.** The mean values of  $v_{max}$  (blue),  $F_{max}$  (orange),  $P_{max}$  (green),  $P_B$  (red),  $S_{Fv}$  (purple), and  $d_{Fv}$  (brown) are plotted as a function of the repetition number across the entire RSA test, where the value for each metric is normalized by its initial value obtained in the first repetition. The vertical dashed lines indicate the rest interval between sets, i.e., between repetitions 5 – 6 and 10 – 11. For the purposes of visual clarity, the uncertainties for each datapoint are not shown in this diagram.

11% and 18%, respectively. The  $P_B$  metric had a lower ICC value of 7%, which indicated more athlete uniformity across the average trends of ballistic power and maximum sprint speed throughout the RSA test.

To better visualize the interplay between force- and velocity-orientated  $Fv$  profiles, Figure 4 displays how the specific values of  $F_{max}$  and  $v_{max}$  affect the resulting values of  $d_{Fv}$  and  $S_{Fv}$ . From examination of panel A of Figure 4, it is clear that repetitions with higher values of  $F_{max}$  and  $v_{max}$  resulted in larger  $d_{Fv}$  values. For example, in panel A of Figure 4, the largest  $Fv$ -offsets (i.e., largest  $d_{Fv}$  values) are located in the upper-right portion of the panel where both  $F_{max}$  and  $v_{max}$  values are largest. Similarly, the lowest  $d_{Fv}$  values are associated with reduced  $F_{max}$  and  $v_{max}$  measurements. In particular,  $F_{max}$  appears to have the largest impact on the specific value of  $d_{Fv}$ , since the maximum and minimum values of  $d_{Fv}$  also correspond to the maximum and minimum values of  $F_{max}$ , respectively.

On the other hand, from inspection of panel B of Figure 4, values of  $S_{Fv}$  appear to be less coupled to the specific value of  $v_{max}$  than its  $d_{Fv}$  counterpart. This can be visualized in panel B of Figure 4 through similar  $S_{Fv}$  measurements spanning a large range of  $v_{max}$  values. However, in keeping with panel A of Figure 4, the  $S_{Fv}$  metric appears to be more strongly coupled to the specific value of  $F_{max}$ , although the degree of coupling appears less linear.

In an attempt to better quantify the precise relationships on how  $d_{Fv}$  and  $S_{Fv}$  depend on the values of  $F_{max}$  and  $v_{max}$ , in Figure 5 we display how each metric ( $d_{Fv}$  and  $S_{Fv}$ ) individually relates to their corresponding  $F_{max}$  and  $v_{max}$  values. As

expected, we find that both  $S_{Fv}$  and  $d_{Fv}$  are more strongly influenced by  $F_{max}$  than  $v_{max}$ , which is visually evidenced in Figure 5 by less scatter of the datapoints and steeper gradients of the lines of best fit for the bottom 2 panels. From Figure 5, we can summarize a number of key results:

1. There is a very strong ( $R^2 = 0.76$ ) positive linear relationship between the value of  $d_{Fv}$  and the maximum (mass-)normalized force applied by the athlete (panel C of Figure 5). The low value of ICC (4%) indicates that the linear relationship is robust amongst all participants, regardless of their specific sprint characteristics. Hence, the greater the applied force, the larger the distance between the origin and the line of best fit through the corresponding  $Fv$  curve.
2. There is a strong ( $R^2 = 0.55$ ) positive linear relationship between the value of  $d_{Fv}$  and the maximum sprint speed achieved by an athlete (panel A of Figure 5). While the relationship is evident across all athletes, the ICC value (20%) indicates strong variations in the trends observed between individual athletes. Typically, the greater the maximum sprint speed achieved by an athlete, the larger the distance between the origin and the line of best fit through the corresponding  $Fv$  curve.
3. There is a moderate ( $R^2 = 0.44$ ) negative linear relationship between the value of  $S_{Fv}$  and the maximum (mass-)normalized force applied by the athlete (panel D of Figure 5). The ICC value (13%)

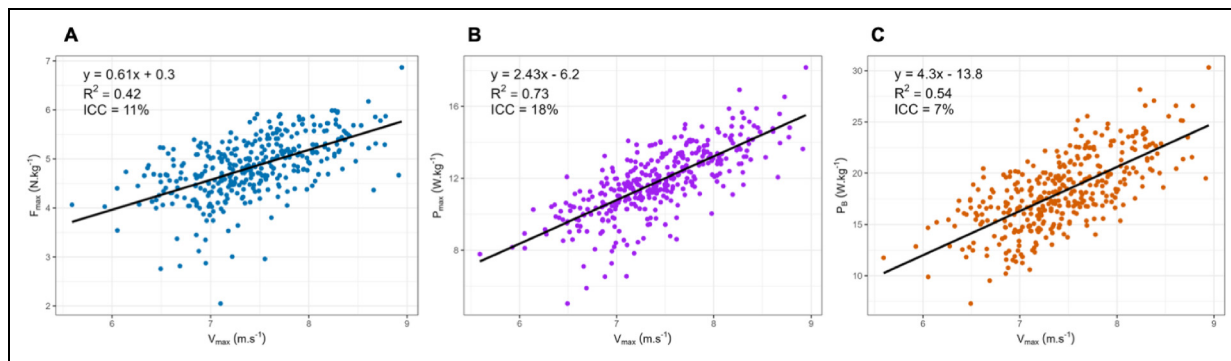


**Figure 3.** Maximum normalized force ( $F_{max}$  in  $N\ kg^{-1}$ ; panel A), maximum power ( $P_{max}$  in  $W\ kg^{-1}$ ; panel B), and ballistic power ( $P_B$  in  $W\ kg^{-1}$ ; panel C) displayed as a function of the maximum athlete velocity ( $v_{max}$  in  $m\ s^{-1}$ ) for each repetition of the RSA test. For each panel, a linear mixed effects model was fitted to the data points, with the corresponding fixed effects model equation, coefficient of determination ( $R^2$ ), and Intraclass Correlation Coefficient (ICC) shown in the upper-left quadrant of each panel.

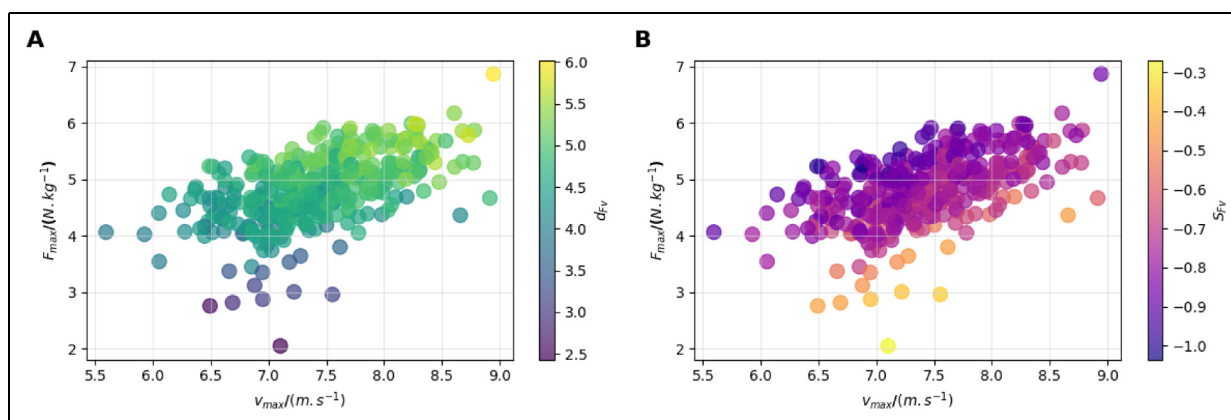


**Figure 4.** Panels A and B show the mass-normalized maximum force ( $F_{max}$  in units of  $N\ kg^{-1}$  or  $m\ s^{-2}$ ) displayed as a function of the maximum speed ( $v_{max}$ ) obtained during each repetition of the RSA test for all 24 participating subjects. In panel A, the datapoints are colored by the value of the  $Fv$ -offset ( $d_{Fv}$ ), while panel B has the datapoints colored by the gradient ( $S_{Fv}$ ) of the line of best fit applied to each of the  $Fv$  curves.

indicates some variation in the trends between individual subjects. Here, the larger the applied force, the more negative the associated gradient is for the line of best fit through the corresponding  $Fv$  curve.

- There is a weak (if any;  $R^2 = 0.32$ ) correlation between the value of  $S_{Fv}$  and the maximum sprint speed achieved by an athlete. From inspection of panel B of Figure 5, the datapoints appear uncorrelated, hence the  $R^2 = 0.32$  initially seems too large. However, 94% of this  $R^2$  value is accounted for by the differences seen between individual athletes (i.e., also observed through the relatively large ICC value of 30%), and therefore this measure is not representative of the average group characteristics. Here, the gradient of the line of best fit through the corresponding  $Fv$  curve appears to have no dependency on the maximum sprint speed achieved by the athlete.

Finally, Figure 6 displays  $F_{max}$  (Panel A) and  $v_{max}$  (Panel B) values as a function of the ballistic power,  $P_B$ . Here, we find a strong linear correlation between the maximum force and the ballistic power ( $R^2 = 0.86$ ; panel A) and moderate linear correlation between the maximum athlete speed and the ballistic power ( $R^2 = 0.68$ ; panel B). As a result, the ballistic power,  $P_B$ , is able to encapsulate information linked to force *and* velocity profiling in a single metric due to the positive linear correlations highlighted in Figure 6.

### Potential psychological factors

From visual inspection of Figure 2, most metrics seem to produce an ‘elbow’ in the transition between the fourth and fifth repetitions of each set, where the percentage value actually increases slightly during the final repetition of a given set. This tendency is most visible between repetitions 9 – 10, and to a lesser degree between repetitions 4 – 5 and

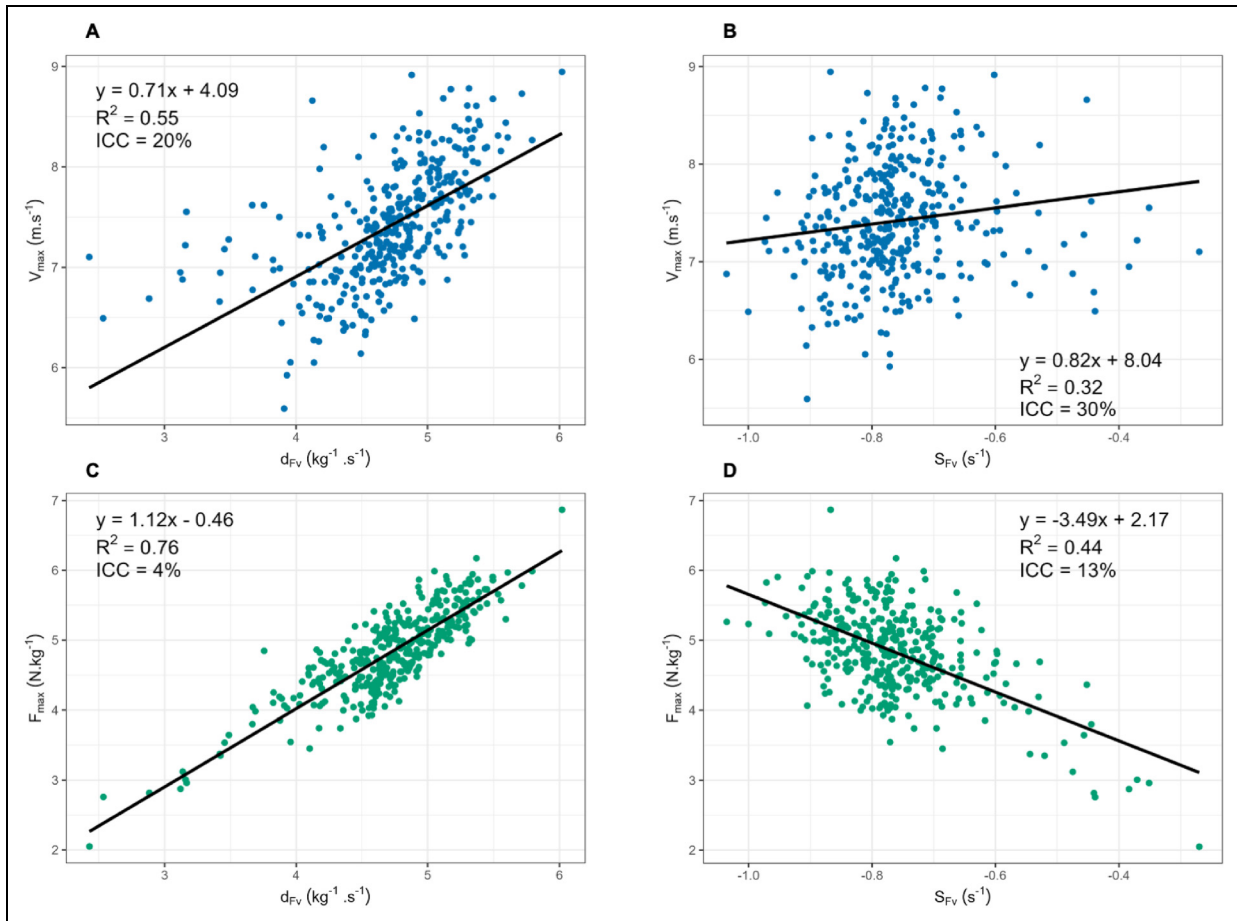


**Figure 5.** Scatter plots displaying the dependency of an athlete's maximum sprint speed ( $v_{\max}$ ; top row, A and B) and maximum applied force ( $F_{\max}$ ; bottom row, C and D) on the  $Fv$ -offset ( $d_{Fv}$ ; left column) and the gradient of the line of best fit through the corresponding  $Fv$  curve ( $S_{Fv}$ ; right column) metrics. Linear mixed effects models were fitted to the datapoints, with the corresponding fixed effects equation, coefficient of determination ( $R^2$ ), and Intraclass Correlation Coefficient (ICC) listed in the corner of each panel.

14 – 15. Although not interpreted as empirical evidence, this trend may suggest a psychological factor at play between the penultimate and final repetitions of each sprint set. As such, this exploratory observation should be considered as an area for further investigation in follow-up *RSA* tests, including those incorporating diverse ages and genders.

## Discussion

### Relationships between speed, force, and power outputs

As revealed in the Results section, we find that the value of  $P_{\max}$  occurs at progressively lower speeds throughout the *RSA* test. This implies that the speed at which an athlete produces peak power reduces with fatigue (i.e.,  $4.46 \pm 0.17 \text{ m}\cdot\text{s}^{-1}$  in repetition 1, compared with  $3.99 \pm 0.22 \text{ m}\cdot\text{s}^{-1}$  in repetition 15, providing an  $\sim 11\%$  reduction in the athlete speed corresponding to peak power).

The approximately linear relationships displayed in Figure 3 suggest that athletes with high velocity capabilities (i.e., a relatively high  $v_{\max}$ ) also possess higher force and power production capabilities. From examination of an athlete's power-velocity profiles (e.g., the solid purple curve in Figure 1B), low values of kurtosis suggest that the peak of the power-velocity curve is relatively flat, enabling high power to be maintained across a broader velocity interval before beginning to reduce.

The slope of the force-velocity curve,  $S_{Fv}$  (solid orange line in Figure 1B), represents an index of an athlete's individual balance between their force and velocity outputs, whereby a more negative  $S_{Fv}$  value (i.e., a steeper gradient) indicates a more force-orientated  $Fv$  profile<sup>15</sup> that is represented by a large applicable force, yet a relatively low maximum speed. Conversely, a less steep  $S_{Fv}$  value indicates a more velocity-orientated  $Fv$  profile that is represented by a relatively high maximum sprint speed, albeit with a reduced amount of applicable force.

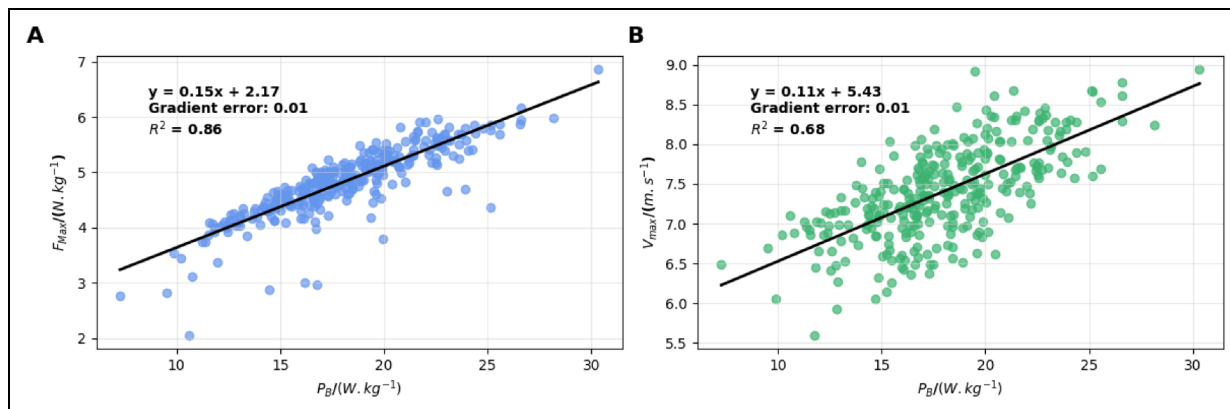


**Figure 6.** Scatter plots displaying the mass-normalized maximum applied force ( $F_{\max}$ ; panel A) and maximum sprint speed ( $v_{\max}$ ; panel B) as a function of the ballistic power,  $P_B$ . Linear lines of best fit are applied to each of the scatter plots, with the corresponding best fit equation, gradient uncertainty, and coefficient of determination ( $R^2$ ) listed in the upper-left corner of each panel.

Figure 3 indicates that while there are similar overall trends between the maximum force, the maximum power, and the ballistic power generated by athletes as a function of maximum sprint speed, the lower ICC value of 7% that is associated with  $P_B$  indicates more athlete uniformity across the average trends of ballistic power (when compared to their maximum force and maximum power counterparts) observed throughout the *RSA* test.

### $S_{Fv}$ and sprint performance

There is a very weak correlation between the slope of the force-velocity profile,  $S_{Fv}$ , and an athlete's maximum sprint speed,  $v_{\max}$ , as shown in panel B of Figure 5. As a result, we suggest that accurate interpretation of calculated  $S_{Fv}$  values may require athlete-specific investigations, especially since the relatively large ICC value (30%) highlights how the statistical behavior is significantly dependent on an individual athlete's sprint characteristics.

Instead, we propose that the novel  $d_{Fv}$  metric, which is the shortest distance between the origin and the linear line of best fit through the athlete's corresponding  $Fv$  data (i.e., the  $Fv$ -offset), acts as a more useful indicator of overall sprint performance than its  $S_{Fv}$  counterpart. This is a result of the strong interplay between both the maximum sprint speed ( $v_{\max}$ ) and the maximum force applied ( $F_{\max}$ ) by the athlete to the final value of the  $d_{Fv}$  metric, as indicated by the strong positive linear relationships in panels A and C of Figure 5. Hence, the  $d_{Fv}$  parameter may help sprint (and subsequent fatigue) analysis remain independent of additional athlete characteristics that are not directly related to their  $F_{\max}$  and  $v_{\max}$  metrics.

### $P_B$ as an indicator of neuromuscular fatigue

Figure 2 suggests that measures of power (i.e.,  $P_{\max}$  and, in particular,  $P_B$ ) have greater sensitivity to fatigue than more

simplistic velocity magnitudes, perhaps due to the power values depending on both the force and the velocity at which it is applied. Across the first 10 repetitions,  $P_{\max}$  reduces to slightly lower values than our proposed ballistic power ( $P_B$ ) metric. However, in the final set, where players are clearly under more physical stress due to the previous 10 repetitions,  $P_B$  values are consistently lower across all 5 repetitions of the final set, hence highlighting its importance as an indicator of longer-term (longitudinal) neuromuscular fatigue. Due to the  $S_{Fv}$  measure not showing clear degradation in Figure 2 with each successive repetition and/or set of the *RSA* test, we do not consider it as an accurate indicator of athlete fatigue.

As seen in Figure 2, fatigue can be observed across multiple measurements during the *RSA* test.  $PFv$  metrics, including parameters linked to the maximum sprint speed ( $v_{\max}$ ), maximum applied force ( $F_{\max}$ ), the peak athlete power ( $P_{\max}$ ), and the newly defined ballistic power ( $P_B$ ), all displayed fatigue-based evolution as an overall percentage decrease of the relevant metric following the first repetition of the *RSA* test. Specifically, the  $v_{\max}$ ,  $F_{\max}$ ,  $P_{\max}$ , and  $P_B$  variables decreased by up to 17.1%, 19.7%, 29.3%, and 31.8%, respectively, across the *RSA* test. Based on these results, it appears that the ballistic power,  $P_B$ , is best suited to detect the effects of longitudinal neuromuscular fatigue when considered among other  $PFv$  related outputs.

As one might expect, there are noticeable recoveries between sets (i.e., between repetitions 5 – 6 and 10 – 11) when the athletes have an extra 02:30 recovery time available to them. Figure 2 suggests that measures of power (i.e.,  $P_{\max}$  and, in particular,  $P_B$ ) have greater sensitivity to fatigue than more simplistic velocity magnitudes, perhaps due to the power values depending on both the force and the velocity at which it is applied.

As can be seen in Figure 2,  $P_B$  is more sensitive to fatigue than  $P_{\max}$ . This may be a consequence of  $P_B$  representing the full extent of the ballistic motion (i.e., the area

under the  $Fv$  curve) rather than a single maximal data point (i.e., the turning point of the power-velocity curve). As such, the greater sensitivity of the  $P_B$  metric to athlete fatigue may enable more representative understanding of an individual's sprint performance. Furthermore, the  $P_B$  metric may also more reliably help identify growing fatigue within an athlete than other (less responsive) measures associated with  $PFv$  analysis.

It must be highlighted that the minimum velocity value,  $v_{\min}$ , used in the definition of the ballistic power,  $P_B$  (Equation 1), was selected to be the first velocity measurement of an athlete's sprint that was  $>0.25 \text{ m s}^{-1}$ . This threshold was chosen due to all athletes commencing their *RSA* test from an approximate standing start. However, we propose that the sensitive nature of the ballistic power to athlete fatigue means it can be universally applied to real-time situations involving invasive team sports and endurance events. Here, it is unlikely that all ballistic movements will be started from an almost stationary position. For example, soccer players may undertake an explosive sprint while already moving within a low-speed running environment, or cyclists may perform a rapid sequence of acceleration to overtake a fellow competitor while already moving at a cruising speed. As such, the  $v_{\min}$  value can be carefully refined to be sport and/or context specific, hence ensuring its accuracy and reliability as a real-time fatigue indicator across a wide variety of sports.

The reduction observed in  $P_B$  is likely a result of changes in magnitude and orientation of the athletes' application of force following neuromuscular and contractile changes over the course of the *RSA* test. Fatigue compromises not only the ability to produce force, but the effectiveness of the application on that force in the horizontal direction.<sup>57</sup> Further to this, acute fatigue has been shown to concurrently decline maximum force and velocity capacities, shifting the  $Fv$  curve downwards.<sup>58</sup> These factors contribute to a sub-optimal mechanical profile and a corresponding reduction in mechanical power.<sup>14</sup> Considering these factors,  $P_B$  appears to provide a reflection of neuromuscular fatigue that integrates the findings of Morin et al.,<sup>57</sup> Cross et al.,<sup>58</sup> and Samozino et al.,<sup>14</sup> rather than acting as a direct measure of sprint performance, which supports its potential as an active fatigue monitor in applied settings.

Following on from the discussions above, while  $P_B$  appears to be the most sensitive metric to *RSA* test-induced fatigue, what is currently unknown is whether measurements of the ballistic power can have a significant impact on *RSA* performance outcomes. Commonly, attenuation in sprint performance is monitored by a number of variables, including distance covered, time to completion in a set run, maximum speed reached, etc. However, we propose that the  $P_B$  measurements may be an alternative, more sensitive measure of performance based on the outcomes of the mixed effects

models, hence may be able to help refine training protocols, ultimately benefiting the performance outcomes of *RSA* tests. Future work should compare  $P_B$  measurements from *RSA* testing protocols that vary recovery times between sprint efforts, with the recovery time that showcases the smallest degradation in  $P_B$  guiding practitioners when prescribing repeated sprint training. Similarly, future work should also include measurements of  $P_B$  using testing protocols analogous to velocity-based training,<sup>59</sup> whereby loads and/or recovery times are adjusted on a set-by-set basis to better understand the sensitivity of ballistic power measurements to *RSA* tests.

This study has investigated the response of several traditional and novel  $PFv$  metrics. We note that the  $d_{Fv}$  metric, while showing potential to indicate shifts in the force-velocity relationship, when compared to other  $PFv$ -derived metrics (such as the ballistic power,  $P_B$ ) is not a sensitive representation of neuromuscular fatigue.

### *Elbow effect – discussing psychological influence*

Most of the metrics displayed in Figure 2 produce an 'elbow' in the transition between the penultimate and final repetitions of each set, where the percentage value unexpectedly increases slightly during the final repetition of a given set. A similar effect has been observed in previous *RSA* testing programs,<sup>60</sup> although no reasons for this distinctive characteristic were put forward by the authors.

While we cannot interpret the performance 'elbow' between fourth and fifth repetitions in each set of the *RSA* test as empirical evidence, we propose the importance of follow-up studies to investigate the presence of any underlying psychological reasons for this trend, whereby the athletes may be aware that the fifth repetition will be their last before a short rest period, hence they may exert themselves more in the final repetition, knowing that they will be able to rest once it is completed. Such psychological manifestations often come under the label 'sandbagging', which has been observed in a number of explosive sports,<sup>61,62</sup> including high school and college athletics,<sup>63,64</sup> cycling,<sup>65</sup> and soccer.<sup>66</sup>

## **Practical Applications**

### *Real-time fatigue monitoring using GPS data*

Athletes using GPS devices, during both training and match scenarios, are able to have  $P_B$  metrics tracked in real-time. Practitioners should take repeated  $P_B$  measurements for each athlete, comparing them to both personal baseline values and team-wide trends. A significant drop in  $P_B$  during maximal (or near-maximal) efforts may indicate fatigue, warranting considerations of adjusted

workload; both immediately and over time. For invasive team sports, decreases in ballistic power measurements will also provide coaching staff with real-time athlete and team fatigue levels, helping them make informed decisions regarding substitutions and/or formation changes.

In training environments, the implementation of our  $P_B$  methods may be somewhat analogous to the use of velocity-based training (VBT<sup>59,67</sup>), which has been shown to help induce neuromuscular adaptations and reduce fatigue through the adjustment of applied loads based on specific velocity movements. The heightened sensitivity of power-based measurements (e.g.,  $P_B$ ) may help enable better granularity in fatigue identification, where the principles may also be applied universally across all ballistic movements, such as sprinting, team sports, Olympic lifting, and plyometrics, including both in training and during real-time match conditions. Hence, establishing a value corresponding to the smallest worthwhile change (SWC) would enable better identification of individual athlete fatigue. However, the present study is a proof-of-concept to showcase the ability of a novel new metric, ballistic power ( $P_B$ ), to respond to the neuromuscular fatigue of athletes involved in RSA testing protocols. Therefore, we recommend that follow-up, comprehensive studies (e.g., taking into account larger, more diverse sample sizes and/or exploring the real-time feasibility of this metric) are performed to estimate the SWC linked to individual athlete fatigue, which would enable a robust load management decision tree to be constructed for coaches, instructors, and practitioners alike.

Although the  $d_{Fv}$  metric captures shifts in the force-velocity relationship, short-term training or monitoring decisions may not be best based on this metric alone. Instead, we proposed that the  $d_{Fv}$  metric can be employed as a complementary tool alongside traditional  $PFv$  metrics to provide a more complete view of changes in individual  $PFv$  profiles. Furthermore, as a long-term tool, the  $d_{Fv}$  metric may help showcase the development of youth athletes since physiological changes and growth may potentially manifest as increases in both the maximum applied force and the maximum achieved velocity of the athlete, which would be collectively represented by an increase in the  $d_{Fv}$  magnitude.

### Implementing repeated GPS-based sprint profiling

Data from maximal (or near-maximal) efforts can be used to build a historical record of  $PFv$  profiles. This database serves as a reference point for tracking player development and identifying performance trends. Furthermore, in return-to-play protocols, an athlete's past  $PFv$  data can provide an ideal visionary benchmark, ensuring they regain pre-injury sprint capacity before returning to competition.

### Strengths

Traditionally,  $PFv$  metrics have been used to evaluate neuromuscular power production in athletes.  $PFv$  metrics have been shown to be reliably produced using GPS/GNSS data in both isolated maximal sprint efforts, as well as using large amounts of data collected in-situ during training and matches.<sup>68</sup> However, these methods have drawbacks, notably in how dedicated testing protocols impose on practitioners and players, often requiring specialized technology and expertise,<sup>25</sup> and in how in-situ methods require a large volume of data to generate sufficient number statistics.<sup>10</sup> Here, we introduce novel new metrics – in particular, the ballistic power,  $P_B$  – which offers a multitude of benefits over traditional  $PFv$  values, which we summarize as:

1.  $P_B$  is directly correlated with traditional  $PFv$  metrics, such as the maximum applied force ( $F_{max}$ ) and maximum sprint speed ( $v_{max}$ ), as demonstrated in Figure 6. The high  $R^2$  values observed in both panels of Figure 6 highlight that the ballistic power,  $P_B$ , is able to encapsulate information linked to force and velocity profiling in a single metric.
2.  $P_B$  is more sensitive to neuromuscular fatigue than other  $PFv$  metrics (see Figure 2), hence ensuring that  $P_B$  captures athlete performance degradation more readily than other  $PFv$ -based variables.
3.  $P_B$  can be calculated via a simple mathematical relationship (see Equation 1), ensuring computational efficiency. Such processing simplicity allows real-time computation from wearable GPS data that can be performed via modern solutions such as cloud computing, which can be integrated into existing technologies for immediate fatigue assessment during training sessions or matches.
4. Derivation of  $P_B$  values no longer relies upon the significant accumulation of large numbers of data-points during matches (i.e., to ensure the  $Fv$  profile is accurately compiled), or the time consuming implementation of dedicated sprint sessions during training. Instead,  $P_B$  can be calculated from individually identified sprints occurring in both matches and training sessions alike, hence providing an efficient and streamlined way to examine time-dependent aspects of athlete fatigue.

As highlighted above, the present study introduces a new method for quantitatively assessing an athlete's capacity to perform repeated explosive movements, hence demonstrating itself as a valuable tool for guiding training practices and assessing performance outcomes. While the methods outlined here focus on sprint running, they may be applied to any explosive motion where velocity and acceleration variables are measurable. The data collection process may

also be adapted for different sports, as well as for adolescent or less physically conditioned athletes.

## Limitations

The study presented here employed 24 sub-elite, physically active males. As a consequence, the results described may not translate perfectly to the broader athletic population, including female athletes, elite professionals, and adolescents. As such, further development and refinement of our presented methods should be performed in follow-up studies linked to more diverse pools of athletes. Additionally, as the work presented here is an exploratory investigation, it was not possible to undertake an a-priori study of ballistic power signatures. Instead, we have utilized post-hoc analyses of effect sizes (e.g., through examination of Cohen's  $d$  values) to examine how our new metrics, notably the ballistic power, link to athlete fatigue.

The methods presented here were devised through the use of a *RSA* test, which is more relevant to sports with intermittent activity levels than, e.g., endurance or strength-biased sports. In addition, the *PFv* profiles do not fully capture non-linear movement patterns, reactive decelerations or multi-directional running, so future work may require vector (i.e., two-dimensional) velocity information to be incorporated into the methodology. Thankfully, the methods presented here utilize GPS data, so motion vectorization is entirely possible, although the reliability of such data can be affected by environmental conditions so needs to be treated carefully. Finally, the data collected during the *RSA* test only accounts for fatigue caused by locomotion and, hence, does not measure any physiological variables or additional fatigue factors such as mental stress, physical contact, game-specific intensity levels, etc., which are regularly faced in real-world scenarios. Accounting for these additional variables will likely require consultation with trained mental wellbeing professionals and muscular-skeletal consultants, in addition to higher-level mixed effects modeling.

Finally, this study focuses on acute fatigue during a single *RSA* testing session, hence the replication of results may be somewhat affected by the sub-elite sample of participants, (small) errors associated with GPS units, and possible unknown environmental factors from the outdoor testing environment. Despite any potential limitations, the novel metrics,  $P_B$  and  $d_{Fv}$ , show promise as tool for real-time fatigue monitoring and should be benchmarked further in future data investigations.


## Conclusion

During our investigation, we put forward two new metrics for consideration, notably the shortest (perpendicular) distance from the origin to the line of best fit through an athlete's *Fv* data,  $d_{Fv}$  (or the *Fv*-offset), and the ballistic

power,  $P_B$ , defined in Equation 1 as the area under the corresponding *Fv* profile.  $d_{Fv}$  is a metric that can be used in tangent with the existing  $S_{Fv}$  measurement, which is the gradient of the line of best fit applied to an athlete's *Fv* curve. As shown in Figure 4,  $d_{Fv}$  appears to be more sensitive to overall *Fv* profiles than its  $S_{Fv}$  counterpart due to increased sensitivities to both the maximum force ( $F_{max}$ ) and velocity ( $v_{max}$ ) values of the associated sprint. As such, the *Fv*-offset ( $d_{Fv}$ ) is likely to be a more useful indicator of overall sprint performance than its *Fv* gradient ( $S_{Fv}$ ) counterpart. Importantly, the ballistic power metric,  $P_B$ , has been shown to be the most reactive to fatigue, hence is likely to be an important parameter for athletes, coaches, and sports practitioners alike in the examination of short- and long-term fitness metrics. However there should be further investigations undertaken into the applicability of these methods in professional/elite cohorts and within female and youth athletes, as well as how these metrics may be applied in real-time situations to assist with aspects such as substitution recommendations in invasive team sports.

Future studies should examine the practical utility of  $P_B$  in performance settings, specifically whether training programs informed by  $P_B$  responses lead to improved training adaptation, reduced injury risk, and/or increased player readiness. A key research question will be determining the SWC in  $P_B$  that will require intervention by performance staff.

## ORCID iD

Eamon McGleenan  <https://orcid.org/0009-0006-8027-781X>

## Ethics approval and informed consent

Written, informed consent was obtained from the participants and the study was approved by the Engineering and Physical Sciences Faculty Research Ethics Committee of Queen's University Belfast (reference number: EPS 24\_48).

## Author Contributions

EMcG conceptualized the study, conducted a literature search, collected and analyzed the data, and wrote the original version of the manuscript; SDTG assisted with the data processing, ethical reporting, and pseudonymization of the data products; LHMcf performed statistical analysis and supported the paper draft; JCJB advised on statistical analysis during the editorial process; JWS contributed to the project narrative and supported the drafting of the manuscript; TdMM supported the research via industry liaison with STATSports, provided guidance on data handling and processing, and contributed to manuscript revisions; RM assisted by advising on data collection techniques and providing invaluable software troubleshooting; DBJ supervised the research, obtained supportive research funding awards, managed the project, advised on the data analysis, and contributed to the manuscript. All authors contributed to interpreting data, have read and

approved the final version of the manuscript, and agree with the order of presentation of the authors.

### Funding details

The author(s) disclosed receipt of the following financial support for the research, authorship, and/or publication of this article: This work was supported by the Northern Ireland Department for the Economy under the Co-operative Awards in Science and Technology (CAST) Grant; the UK Science and Technology Facilities Council (STFC) under Grants ST/T00021X/1 and ST/X000923/1; and the UK Engineering and Physical Sciences Research Council (EPSRC) under their Impact Acceleration Award Grant.

### Declaration of conflicting interests

The authors declared no potential conflicts of interest with respect to the research, authorship, and/or publication of this article.

### Availability of data and materials

The data that support the findings of this study are available on reasonable request from one of the co-authors, SDTG.

### Code availability statement

The code used for the statistical analysis presented in this paper will be made under reasonable request to the corresponding author.

### Disclosure statement

The authors declare that they have no competing interests.

### Notes

1. Apex Pro series unit, STATSports, Newry, Northern Ireland
2. Sonra Version 5.0.6, STATSports, Newry, Northern Ireland

### References

1. Weavil JC and Amann M. Neuromuscular fatigue during whole body exercise. *Curr Opin Physiol* 2019; 10: 128–136.
2. Carling C, Lacombe M, McCall A, et al. Monitoring of post-match fatigue in professional soccer: welcome to the real world. *J Sports Med* 2018; 48: 2695–2702.
3. Buchheit M and Simpson BM. Player-tracking technology: half-full or half-empty glass? *Int J Sports Physiol Perform* 2017; 12: S2–S35.
4. Mohr M, Krstrup P, Nybo L, et al. Muscle temperature and sprint performance during soccer matches—beneficial effect of re-warm-up at half-time. *Scand J Med Sci Sports* 2004; 14: 156–162.
5. Mohr M, Krstrup P and Bangsbo J. Fatigue in soccer: a brief review. *J Sport Sci* 2005; 23: 593–599.
6. Mohr M, Krstrup P, Andersson H, et al. Match activities of elite women soccer players at different performance levels. *J Strength Cond Res* 2008; 22: 341–349.
7. Rampinini E, Coutts AJ, Castagna C, et al. Variation in top level soccer match performance. *Int J Sports Med* 2007; 28: 1018–1024.
8. Hader K, Rumpf MC, Hertzog M, et al. Monitoring the athlete match response: Can external load variables predict post-match acute and residual fatigue in soccer? a systematic review with meta-analysis. *Sports Med Open* 2019; 5: 48.
9. Pimenta R, Cunha L and Nakamura FY. Impact of post-match fatigue on peak force in elite youth soccer players: Analysis of 48 to 72 hours post-match using the isometric mid-thigh pull exercise. *Biol Sport* 2025; 42: 145–152.
10. Morin JB, Le Mat Y, Osgnach C, et al. Individual acceleration-speed profile in-situ: A proof of concept in professional football players. *J Biomech* 2021; 123: 110524.
11. Snyder BJ, Maung-Maung C and Whitacre C. Indicators of fatigue during a soccer match simulation using gps-derived workload values: which metrics are most useful? *Sports* 2023; 12: 9.
12. Rabita G, Dorel S, Slawinski J, et al. Sprint mechanics in world-class athletes: a new insight into the limits of human locomotion. *Scand J Med Sci Sports* 2015; 25: 583–594.
13. Haugen TA, Breitschädel F and Samozino P. Power-force-velocity profiling of sprinting athletes: methodological and practical considerations when using timing gates. *J Strength Cond Res* 2020; 34: 1769–1773.
14. Samozino P, Peyrot N, Edouard P, et al. Optimal mechanical force-velocity profile for sprint acceleration performance. *Scand J Med Sci Sports* 2022; 32: 559–575.
15. Morin JB and Samozino P. Interpreting power-force-velocity profiles for individualized and specific training. *Int J Sports Physiol Perform* 2016; 11: 267–272.
16. Alba-Jiménez C, Moreno-Doutres D and Peña J. Trends assessing neuromuscular fatigue in team sports: a narrative review. *Sports* 2022; 10: 33.
17. Rampinini E, Sassi A, Morelli A, et al. Repeated-sprint ability in professional and amateur soccer players. *Appl Physiol Nutr Metab* 2009; 34: 1048–1054.
18. Bishop D and Edge J. Determinants of repeated-sprint ability in females matched for single-sprint performance. *Eur J Appl Physiol* 2006; 97: 373–379.
19. Bishop D, Girard O and Mendez-Villanueva A. Repeated-sprint ability—part ii: recommendations for training. *J Sports Med* 2011; 41: 741–756.
20. Dawson B. Repeated-sprint ability: where are we? *Int J Sports Physiol Perform* 2012; 7: 285–289.
21. Gonzalez-Custodio A, Crespo C, Timón R, et al. Effects of a combined method of normobaric hypoxia on the repeated sprint ability performance of a nine-time world champion triathlete: A case report. *Behav Sci* 2024; 14: 1084.
22. Girard O, Mendez-Villanueva A and Bishop D. Repeated-sprint ability—part i: factors contributing to fatigue. *J Sports Med* 2011; 41: 673–694.
23. Morin JB, Samozino P, Edouard P, et al. Effect of fatigue on force production and force application technique during repeated sprints. *J Biomech* 2011; 44: 2719–2723.
24. Cormie P, McGuigan MR and Newton RU. Developing maximal neuromuscular power: Part 1—biological basis of maximal power production. *J Sports Med* 2011; 41: 17–38.

25. Cross MR, Brughelli M, Samozino P, et al. Methods of power-force-velocity profiling during sprint running: a narrative review. *J Sports Med* 2017; 47: 1255–1269.
26. Lipčák A, Lipková L, Kalina T, et al. The use of horizontal force-velocity profile in soccer: a rapid systematic review. *BMC Sports Sci Med Rehabil* 2025; 17: 200.
27. Abt G, Siegler JC, Akubat I, et al. The effects of a constant sprint-to-rest ratio and recovery mode on repeated sprint performance. *J Strength Cond Res* 2011; 25: 1695–1702.
28. Jeffreys I. Ramp warm-ups: more than simply short-term preparation. *PSCJ* 2017; 44: 17–23.
29. Thurlow F, Huynh M, Townshend A, et al. The effects of repeated-sprint training on physical fitness and physiological adaptation in athletes: a systematic review and meta-analysis. *J Sports Med* 2024; 54: 953–974.
30. Daly LS, Catháin CÓ and Kelly DT. Gaelic football match-play: performance attenuation and timeline of recovery. *Sports* 2020; 8: 166.
31. Plakias S. Running performance profiles of different types of central midfielders in soccer. *Trends Sport Sci* 2025; 32: 26.
32. Tierney P, Blake C and Delahunty E. Physical characteristics of different professional rugby union competition levels. *J Sci Med Sport* 2021; 24: 1267–1271.
33. Van Rossum G and Drake FL. *Python 3 Reference Manual*. Scotts Valley, CA: CreateSpace, 2009.
34. Beato M, Coratella G, Stiff A, et al. The validity and between-unit variability of gnss units (statsports apex 10 and 18 hz) for measuring distance and peak speed in team sports. *Front Physiol* 2018; 9: 9.
35. Scott MT, Scott TJ and Kelly VG. The validity and reliability of global positioning systems in team sport: a brief review. *J Strength Cond Res* 2016; 30: 1470–1490.
36. Cormier P, Tsai MC, Meylan C, et al. Concurrent validity and reliability of different technologies for sprint-derived horizontal force-velocity-power profiling. *J Strength Cond Res* 2023; 37: 1298–1305.
37. Imano M, Kido M, Honsho C, et al. Assessment of directional accuracy of gnss-acoustic measurement using a slackly moored buoy. *Prog Earth Planet Sci* 2019; 6: 56.
38. pandas development team T. pandas-dev/pandas: Pandas, 2020. DOI: 10.5281/zenodo.3509134.
39. Jess DB, Jafarzadeh S, Keys PH, et al. Waves in the lower solar atmosphere: the dawn of next-generation solar telescopes. *Living Rev Sol Phys* 2023; 20: 1.
40. Virtanen P, Gommers R, Oliphant TE, et al. SciPy 1.0: Fundamental algorithms for scientific computing in python. *Nat Methods* 2020; 17: 261–272.
41. Cafiso S, Di Graziano A, Giudice O, et al. Using gps data to detect critical events in motorcycle rider behaviour. *Int J Mobile Network Des Innov* 2014; 5: 195–204.
42. Thoseby B, Govus AD, Clarke A, et al. Positional and temporal differences in peak match running demands of elite football. *Biol Sport* 2023; 40: 311–319.
43. Delves RI, Duthie GM, Ball KA, et al. Applying common filtering processes to global navigation satellite system-derived acceleration during team sport locomotion. *J Sport Sci* 2022; 40: 1116–1126.
44. Ellens S, Carey DL, Gastin PB, et al. Accuracy of gnss-derived acceleration data for dynamic team sport movements: A comparative study of smoothing techniques. *Appl Sci* 2024; 14: 10573.
45. Harris CR, Millman KJ, van der Walt SJ, et al. Array programming with numPy. *Nature* 2020; 585: 357–362.
46. Nagahara R, Naito H, Morin JB, et al. Association of acceleration with spatiotemporal variables in maximal sprinting. *Int J Sports Med* 2014; 35: 755–761.
47. Nagahara R, Matsubayashi T, Matsuo A, et al. Kinematics of transition during human accelerated sprinting. *Biol Open* 2014; 3: 689–699.
48. Freeman BW, Talpey SW, James LP, et al. Common high-speed running thresholds likely do not correspond to high-speed running in field sports. *J Strength Cond Res* 2023; 37: 1411–1418.
49. Isacson A, Malmgren N and Pendrill AM. Accelerating a car from rest: friction, power and forces. *Phys Educ* 2023; 58: 055005.
50. Haugen T, Danielsen J, Alnes LO, et al. On the importance of “front-side mechanics” in athletics sprinting. *Int J Sports Physiol Perform* 2018; 13: 420–427.
51. Nagahara R and Zushi K. Development of maximal speed sprinting performance with changes in vertical, leg and joint stiffness. *J Sports Med Phys Fitness* 2016; 57: 1572–1578.
52. Haugen T, Seiler S, Sandbakk Ø, et al. The training and development of elite sprint performance: an integration of scientific and best practice literature. *Sports Med Open* 2019; 5: 44.
53. Laird NM and Ware JH. Random-effects models for longitudinal data. *Biometrics* 1982; 38: 963–974.
54. Pinheiro J, Bates D and Core Team R. *nlme: Linear and Nonlinear Mixed Effects Models*, 2025. R package version 3.1-168.
55. Nakagawa S, Johnson PCD and Schielzeth H. The coefficient of determination R<sup>2</sup> and intra-class correlation coefficient from generalized linear mixed-effects models revisited and expanded. *J R Soc Interface* 2017; 14: 20170213.
56. Kianoush F and Masoomehni K. Application REML model and determining cut off of ICC by multi-level model based on markov chains simulation in health. *Indian J Fundam Appl Life Sci* 2015; 5: 1432–1448.
57. Morin JB, Edouard P and Samozino P. Technical ability of force application as a determinant factor of sprint performance. *Med Sci Sports Exerc* 2011; 43: 1680–1688.
58. Cross MR, Samozino P, Brown SR, et al. A comparison between the force-velocity relationships of unloaded and sled-resisted sprinting: single v’s. multiple trial methods. *Eur J Appl Physiol* 2018; 118: 563–571.
59. Włodarczyk M, Adamus P, Zieliński J, et al. Effects of velocity-based training on strength and power in elite athletes—a systematic review. *Int J Environ Res Public Health* 2021; 18: 5257.

60. Wragg CB, Maxwell NS and Doust JH. Evaluation of the reliability and validity of a soccer-specific field test of repeated sprint ability. *Eur J Appl Physiol* 2000; 83: 77–83.
61. Andreff W. Sport manipulations: Breaching sport rules for gaining advantage. In: Andreff W (ed) *An economic roadmap to the dark side of sport. Volume I: sport manipulations*. Cham: Palgrave Pivot, 2019, pp. 29–61.
62. Gibson B and Sachau D. Sandbagging as a self-presentational strategy: Claiming to be less than you are. *Person Soc Psychol Bull* 2000; 26: 56–70.
63. Schatz P, Elbin R, Anderson MN, et al. Exploring sandbagging behaviors, effort, and perceived utility of the impact baseline assessment in college athletes. *Sport, Exerc Perform Psychol* 2017; 6: 243.
64. Tsushima WT, Yamamoto MH, Ahn HJ, et al. Invalid baseline testing with impact: Does sandbagging occur with high school athletes? *Appl Neuropsychol: Child* 2021; 10: 209–218.
65. Dyer B. ‘virtually cycling’: The impact of technology, cheating, and performance enhancement in bicycle e-racing. In: *Social issues in esports*. Routledge, 2022. pp.115–128.
66. Kräkel M. Sandbagging. *J Sports Econom* 2014; 15: 263–284.
67. Orange ST, Hritz A, Pearson L, et al. Comparison of the effects of velocity-based v’s. traditional resistance training methods on adaptations in strength, power, and sprint speed: A systematic review, meta-analysis, and quality of evidence appraisal. *J Sport Sci* 2022; 40: 1220–1234.
68. Cormier P, Tsai MC, Meylan C, et al. Comparison of acceleration-speed profiles from training and competition to individual maximal sprint efforts. *J Biomech* 2023; 157: 111724.